INTERNATIONAL JOURNAL OF PRECISION ENGINEERING AND MANUFACTURING Vol. 19, No. 4, pp. 605-612 APRIL 2018 / 605

REGULAR PAPER

DOI: 10.1007/s12541-018-0073-4
ISSN 2234-7593 (Print) / 2005-4602 (Online)

Comparative Assessment of the Ability of Dual-Pore Structure and Hydroxyapatite to Enhance the Proliferation of Osteoblast-Like Cells in Well-Interconnected Scaffolds

Yong Sang Cho[1], Joon Sup Lee[1], Myoung Wha Hong[3], Se-Hwan Lee[1], Young Yul Kim[3,#], and Young-Sam Cho[2,#]

1 Division of Mechanical and Automotive Engineering, College of Engineering, Wonkwang University, 460, Iksan-daero, Iksan-si, Jeollabuk-do, 54538, Republic of Korea
2 Department of Mechanical Design Engineering, College of Engineering, Wonkwang University, 460, Iksan-daero, Iksan-si, Jeollabuk-do, 54538, Republic of Korea
3 Department of Orthopedics, Daejeon St. Mary's Hospital, Catholic University of Korea, 64, Daeheung-ro, Jung-gu, Daejeon, 34943, Republic of Korea
Corresponding Author / E-mail: kimtwins72@catholic.ac.kr, TEL: +82-42-220-9530, ORCID: 0000-0003-2383-6444
E-mail: youngsamcho@wku.ac.kr, TEL: +82-63-850-6694, ORCID: 0000-0002-0545-1586

KEYWORDS: Tissue engineering, Dual-pore structure, Hydroxyapatite, Wire-network molding, Salt-leaching using powder

In this study, to compare the relative abilities of dual-pore structure and hydroxyapatite to enhance the proliferation of osteoblast-like cell in well-interconnected scaffolds, several types of scaffolds were fabricated using combined SLUP (Salt-Leaching Using Powder) and WNM (Wire-Network Molding) techniques: well-interconnected dual-pore scaffolds with hydroxyapatite particles, well-interconnected dual-pore scaffolds without hydroxyapatite particles, and single-pore scaffolds with hydroxyapatite particles. To assess the characteristics of the fabricated scaffolds, their morphology, compressive modulus, water absorption, and in-vitro cell activity were measured. Consequently, it was found that while the hydroxyapatite (which is hydrophilic) provides some advantage for cell attachment, the cell attachment in the dual-pore scaffold with hydroxyapatite particles was similar to that of the dual-pore scaffold without hydroxyapatite particles. Moreover, regarding cell proliferation, we verified that the effect of the dual-pore structure was dominant compared with the existence of hydroxyapatite particles and co-existence of dual-pore structure/hydroxyapatite particles. However, the cell vitality of the dual-pore scaffold with hydroxyapatite particles was higher than that of the dual-pore scaffold without hydroxyapatite particles because of ions released by the hydroxyapatite particles.

Manuscript received: September 13, 2017 / Revised: October 3, 2017 / Accepted: January 8, 2018

1. Introduction

Tissue engineering is based on developments from multiple fields including life sciences, medical science and engineering. The purpose of tissue engineering is facilitate the maintenance, improvement, and restoration of bio-functions by fabricating biological tissue substitutes that can be used for transplanting.[1-3] To regenerate damaged bone tissue in the human-body, bone tissue engineering utilizes scaffolds with three-dimensional structures to support cells, and certain growth factors. To be effective, the scaffold needs to satisfy several characteristics, including suitable porosity, pore-size, biocompatibility, biodegradability and pore interconnectivity.[4-6] Several conventional methods and solid freeform fabrication (SFF) methods have been proposed to fabricate effective bone regeneration scaffolds. Conventional methods include salt-leaching, solvent casting, phase separation, gas foaming, freeze drying, and electro spinning.[7-12] The solid freeform fabrication (SFF) methods include a stereo lithography apparatus (SLA), selective laser sintering (SLS), and 3D plotting.[13-15]

Recently, dual-pore structures, which are composed of global pores (macro scale) and local pores (meso or micro scale), have been proposed as a strategy for enhancing the cell adhesion and cell proliferation features of bone scaffold materials. According to reported studies, the global pores provide access to oxygen and nutrients while the smaller local pores act as living space for cells.[16,17] Compared with scaffolds having a single-pore structure, the dual-pore structure scaffold has demonstrated improved cell adhesion and proliferation.[18,19]

In the field of bone tissue engineering, bioceramic materials including hydroxyapatite (HA), beta-tri calcium phosphate (β-TCP), and bioactive glass have been utilized to improve cell proliferation, differentiation, and bone regeneration. Generally, bioceramics are known to promote cell proliferation by releasing ions into the in-vitro environment. Moreover, they can enhance osteo-conduction in the in-vivo environment because

of their chemical similarity to natural bone.[20-22] Nonetheless, at the present time, neither the potential synergetic effects of the combination of dual-pore structure and bioceramic materials, or a comparison of their individual effects on cell activity, has been sufficiently investigated. Moreover, there is currently no report on which feature, the dual-pore structure or the bioceramic material, would have the more dominant effect on cell activity in a dual-pore structure/bioceramic material scaffold.

Therefore, in this study, to compare the relative effectiveness of dual-pore structure and hydroxyapatite on enhancing the proliferation of osteoblast-like cells in well-interconnected scaffolds, a dual-pore scaffold with bioceramic material, a dual-pore scaffold without bioceramic material, and a single-pore scaffold with bioceramic material were fabricated via the salt-leaching using powder (SLUP) and wire-network molding (WNM) techniques, which had been proposed in our previous studies.[23,24] Moreover, to exclude the morphological influence of the fabricated scaffolding on cell activity, the dual-pore scaffolds were fabricated using identical fabrication methods and weight ratio of NaCl. Also, the same fabrication method and weight ratio of bioceramic were utilized to fabricate the single-pore scaffold. To prepare the scaffolds this study selected polycaprolactone, which has good processability, cost effectiveness, and relatively high mechanical properties.[25,26] In addition, among various bioceramic materials, we used hydroxyapatite, which exhibits good osteo-conduction characteristics, in the fabrication of the composite scaffold.

2. Materials and Methods

2.1 Material preparation

PCL (Polycaprolactone; Mn= 80,000 Da, Sigma-Aldrich, USA), HA (hydroxyapatite; powder size= from several to ten micrometers, Sigma-Aldrich, USA), sodium chloride (Sigma-Aldrich, USA), and stainless steel needles (STS 304, length= 40 mm, diameter= 500 μm Dongbang Acupuncture, Korea) were prepared to fabricate the scaffold. A stainless-still mold (STS 304) was designed using CATIA V5R19 and produced using a wire-cutting machine. For cell culture experiments, Saos-2 cells were obtained from the American Type Culture Collection (ATCC).

2.2 Preparation of the scaffolds

To fabricate the dual-pore scaffold with HA particles, the dual-pore scaffold without HA particles, and the single-pore scaffold with HA particles using the SLUP and WNM techniques, a stainless steel mold was manufactured (Fig. 1). The mold was composed of four walls with gratings to form the global pores of the scaffold by allowing the insertion of stainless steel needles (diameter = 500 μm). The pitch between the grooves in the walls was 1000 μm and the groove width was 500 μm, respectively. Moreover, each groove was tolerance designed. Each wall of the mold was manufactured with a size of 33 × 20 × 2 mm^3. The bottom cover of the mold was designed to be 24 × 24 × 6 mm^3 to prevent the leakage of the powder composite when the powder composite was inserted into the mold. Furthermore, to pressurize the stainless steel needles so that they maintained intimate contact with each other, the top cover was designed and manufactured with the dimensions 24 × 24 × 14 mm^3. Fig. 1 shows the manufactured mold, top cover, and bottom cover after being assembled.

To obtain the PCL powder (with particle sizes of 63-100 μm), the PCL material was ground using a freezer mill (Freezer/mill 6870, SPEX SamplePrep, USA). Afterward, the PCL powder with 63-100 μm particles was passed through sieves having mesh sizes of 63 μm and 100 μm. Sodium chloride powder was ground using a hand-type ceramic mortar, and after using sieves with 100 μm and 180 μm mesh size, sodium chloride powder with a particle size range of 100-180 μm was obtained. After that, the prepared PCL powder (with particle sizes between 63-100 μm), NaCl powder (with particle sizes between 100-180 μm), and HA powder were mixed at weight ratios of 7:35:3 (PCL:NaCl:HA), 7:35 (PCL:NaCl), and 7:3 (PCL:HA) using a stirrer with a direct driven motor for 3 hours, respectively.

2.3 Fabrication of scaffolds

To fabricate the three types of scaffold (the dual-pore scaffold with HA particles, the dual-pore scaffold without HA particles, and the single-pore scaffold with HA particles), prepared stainless steel needles were inserted into the grooves of the assembled mold (Fig. 1). Subsequently, the mold was filled with the selected prepared composite powder (either PCL:NaCl:HA, PCL:NaCl, or PCL:HA). The top cover was placed onto the top side of the mold and the mold was pressed with 30 MPa for 1 min. After the pressing process, the top cover was removed from the mold and the mold was heated at 100°C for 20 min. After that, the stainless steel needles were removed from the mold and the composite structure was separated from the mold. Subsequently, the fabricated structure was cut into sections of 5 × 5 × 5 mm^3, and these diced scaffolds were soaked in a beaker filled with deionized water. To leach the NaCl out from the composite structure, the beaker was sonicated for 24 h (The water was changed every 6 h),[27-30] and then the composite structure was dried for 24 h in a desiccator.

2.4 Scaffold characterization

To observe the morphological characteristics of the fabricated scaffolds, a field emission scanning electron microscope (FE-SEM, SU8220, Hitachi, Japan) was used. For the morphology analysis, the fabricated scaffolds were coated with platinum for 60 sec. The coated scaffolds were placed on a plate and observed in argon. To confirm the existence of HA particles on the surface of the fabricated scaffolds, a chemical assessment was performed using energy dispersive spectroscopy (EDS; EGX-250, Horiba, Japan). Two scaffolds from each type of scaffold were examined using FE-SEM and EDS.

The porosities of the fabricated scaffolds were calculated using either the following Eqs. (1) or (2). If HA was included, Eq. (1) was adopted. If only PCL was used to fabricate the scaffold, Eq. (2) was adopted. For each type of scaffold, 10 scaffolds were utilized for porosity measurements.

$$Porosity = \frac{V_0 - \left(\frac{0.7 \times m}{\rho_{PCL}} + \frac{0.3 \times m}{\rho_{HA}}\right)}{V_0} \times 100(\%) \quad (1)$$

$$Porosity = \frac{V_0 - \left(\frac{m}{\rho_{PCL}}\right)}{V_0} \times 100(\%) \quad (2)$$

where V_0 is the apparent volume of the scaffold, which is calculated

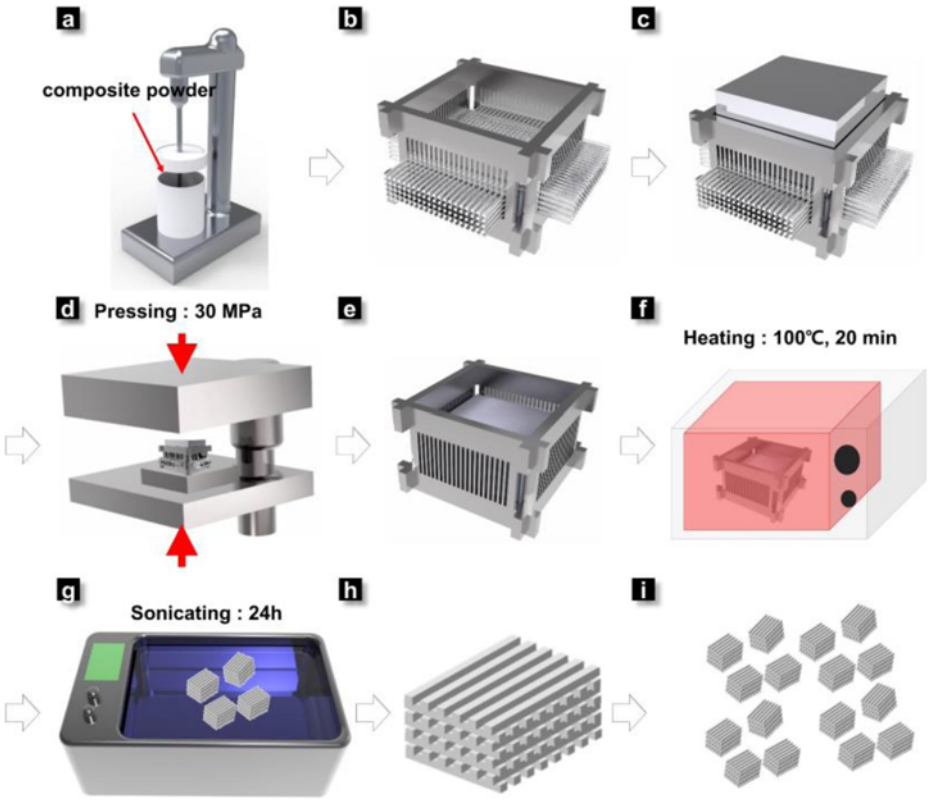

Fig. 1 Schematic of the fabrication process, using a combination of the SLUP (Salt-leaching using powder) and WNM (Wire-network molding) techniques

using the outer dimension of the fabricated scaffolds; m is the mass of the scaffold after salt-leaching; ρ_{PCL} and ρ_{HA} are the densities of PCL and HA.

To measure the compressive modulus of the fabricated scaffolds, a uniaxial compression test was performed using UTM (Z020, Zwick/Roell) at a constant strain rate (1 mm/min) with a 2.5 kN loading cell. Compressive modulus was determined from the initial linear region of the stress-strain curve using the offset method, and 10 scaffolds were assessed for each type of scaffold.[31]

To indirectly assess the cell proliferation ability of each type of scaffold, the level of water absorption of the fabricated scaffolds was measured.[32,33] The fabricated scaffolds were soaked in vials filled with 10 ml of pH 7.4 phosphate-buffered saline (PBS; Gibco, USA) after the scaffold's initial weight was measured. Subsequently, the vials were dipped in a filled water bath (JSWB-22T, JSR, Korea) at 37°C for 12 h. After that, the masses of the three types of soaked scaffolds were measured. The wettability percentage of each type of scaffold were calculated using Eq. (3). For each type, 10 scaffolds were tested.

$$Water\ absorption = \frac{W_{12h} - W_0}{W_0} \times 100(\%) \quad (3)$$

where W_{12h} is the weight of the soaked scaffold after immersion in the PBS solution for 12 h; W_0 is the scaffold's initial weight.

2.5 Cell adhesion and proliferation

After a few passages, cultured Saos-2 cell were detached using EDTA (trypsin ethylenediaminetetra acetic acid) (0.05% w/v trysin and 0.02% w/v EDTA) (Gibco BRL, Grand Island, NY, USA). The scaffolds were sterilized with 70% ETOH overnight under UV light and were washed 3 times using PBS (Phosphate-buffered saline) (Hyclone, USA).

The cell suspensions (cells/20 μl/scaffold) were seeded onto the tops of the pre-wetted scaffolds. The scaffolds were left undisturbed in an incubator for 30 min to allow the cells to attach to the scaffolds. After 30 min, a medium was added and the cells were maintained in DMED supplemented with 10% FBS (Fetal bovine serum) (Hyclone, USA), 1% P/S (100 U/ml penicillin and 100 μg/ml streptomycin) (Gibco BRL, Grand Island, NY, USA), 10 mM beta-glycerophosphate (Sigma), 50 μg/ml L-ascorbic acid (Sigma), and 100 nM dexamethasone (Sigma). The cell culture was maintained at 37°C in a humidified incubator supplemented with 5% CO_2. Half of the medium was changed every 3 days. Analytical assays were performed at 1, 7, and 14 days.

To determine the seeding efficiency and cell growth in the scaffolds, viable cells were measured using the CCK-8 assay kit (Cell Counting Kit-8) (Dojindo, Japan) following the manufacturer's instructions. Absorbance was measured at 450 nm using a microplate reader every 30 min. Cell proliferation data were presented as the mean optical density value from three walls.

2.6 DNA content

To quantify cell proliferation on the scaffolds, the DNA content of cells cultured for 1, 7 and 14 days was measured. Briefly, the cell cultured scaffolds were washed with PBS 3 times, digested overnight at 56°C in proteinase k solution prepared in Tris-EDTA, and then stored at -80°C. The next day, the frozen scaffolds were thawed at room temperature and

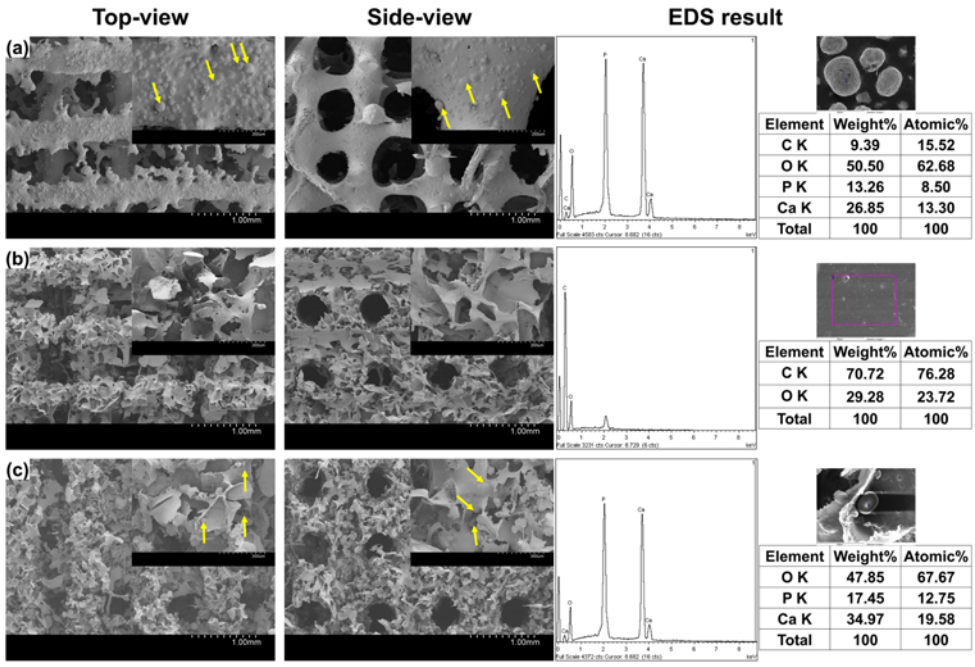

Fig. 2 SEM images (top and side views) and EDS datum of the fabricated composite scaffolds: (a) the single-pore scaffold with HA particles; (b) the dual-pore scaffold without HA particles; (c) the dual-pore scaffold with HA particles. (Yellow arrows: HA particles)

sonicated for 10 sec 5 times to release cellular DNA into the solution. After centrifugation at 13000 rpm for 10 minutes 4°C, the supernatant was transferred into a new tube. DNA content was measured in triplicate using a Nanodrop ND1000 spectrophotometer (NanoDrop Technologies, Wilmington, DE).

2.7 Live and dead assay

The viability of the Saos-2 cells on the scaffolds was evaluated by utilizing a Live/Dead viability kit (Molecular Probes, L-3224). Calcein AM dye, which is green fluorescent, was reacted with the live cells, while ethidium homodimer-1 dye, which is red fluorescent, was reacted with the dead cells. After 7 and 14 days of cultivation, the scaffolds were observed using a fluorescence microscope (Nikon, Japan).

2.8 Statistical analysis

All data are presented as the means±standard deviation. Statistical analysis was conducted by the single factor analyses of variance (ANOVA) using SPSS version 22.0 software (SPSS, IBM Corporation, Chicago, IL, USA). A value of $P<0.05$ was considered statistically significant.

3. Results and Discussion

3.1 Morphological and chemical analyses of the scaffolds

Figs. 2(a)-2(c) shows the top-view images, side-view images, and EDS results of the single-pore scaffold with HA particles, the dual-pore scaffold without HA particles, and the dual-pore scaffold with HA particles, respectively. As shown in Figs. 2(a)-2(c), the dual-pore scaffold with HA particles, dual-pore scaffold without HA particles, and single-pore scaffold with HA particles each have interconnected pores. Moreover, the top-view and side-view images of the dual-pore scaffold with HA particles and the single-pore scaffold with HA particles showed that the HA particles were adhered to the PCL matrix.

Additionally, in the case of the dual-pore scaffold with HA particles and the dual-pore scaffold without HA particles, the dual-pore structure was observed, where global pores were formed by the stainless steel needles, and local pores were formed by leaching out the NaCl particles.

To confirm the presence of HA particles on the fabricated scaffolds, the chemical components of the HA particles were detected using EDS. The chemical compositions of PCL and HA are $(C_6H_{10}O_2)_n$ and $HCa_5O_{13}P_3$, respectively.[34] As shown in Figs. 2(a)-2(c), the Ca and P peaks of the dual-pore scaffold with HA particles and the single-pore scaffold with HA particles were detected. In contrast, in the dual-pore scaffold without HA particles, Ca and P peaks were not detected. Therefore, the existence of HA particles in the dual-pore scaffold with HA particles and the single-pore scaffold with HA particles was confirmed using SEM images and EDS results (Figs. 2(a)-2(c)).

3.2 Porosities, mechanical properties, and water absorption measurement

The porosities of the single-pore scaffold with HA particles, the dual-pore scaffold without HA particles, and the dual-pore scaffold with HA particles were calculated to be 76.2±2.3%, 91.5±0.5%, and 92.6±1.4%, respectively (Fig. 3(a)). The porosities of the fabricated scaffolds were similar to the porosity results obtained in our previous studies.[23,24] Moreover, the porosities of the scaffolds with the dual-pore structure were higher than that of the single-pore scaffold because of the formation of local pores by the leached out NaCl particles.

The mechanical properties of the single-pore scaffold with HA particles, the dual-pore scaffold without HA particles, and the dual-pore scaffold with HA particles were measured to be 7.0±0.7 MPa, 3.4±0.4 MPa, and 3.1±0.2 MPa, respectively. Among the fabricated scaffolds,

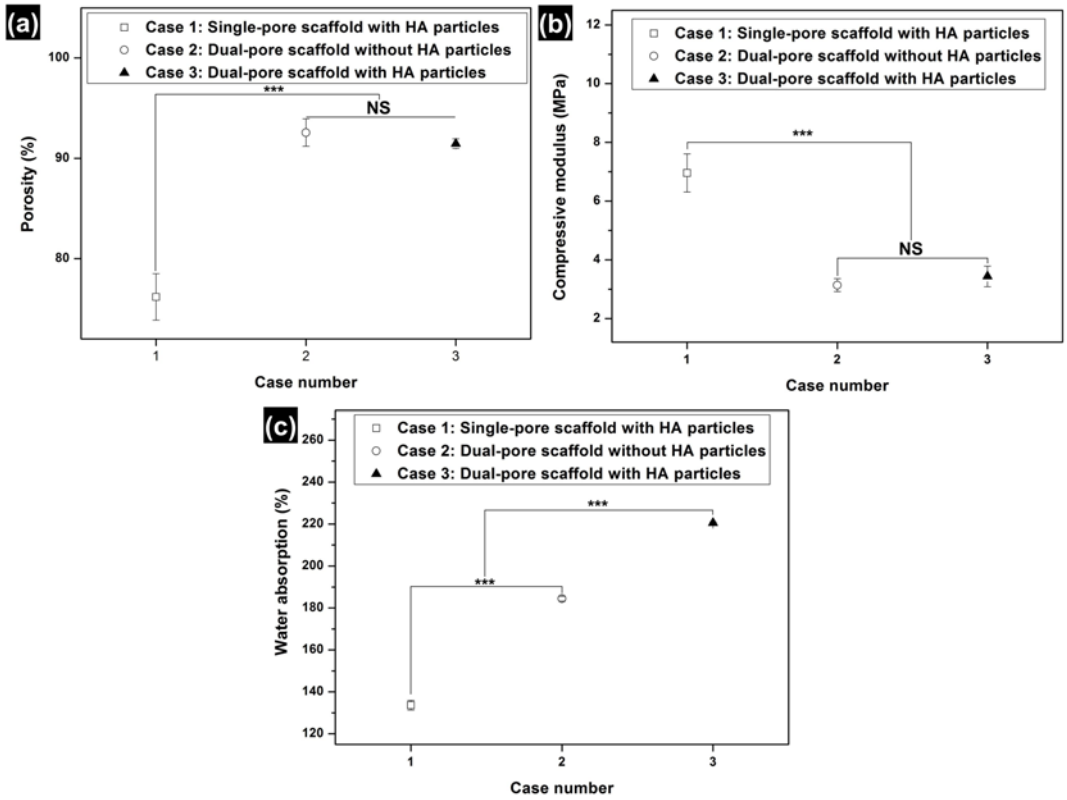

Fig. 3 (a) Porosities, (b) compressive modulus, and (c) water absorption of the fabricated single-pore scaffold with HA particles, dual-pore scaffold without HA particles, and the dual-pore scaffold with HA particles. (***$p < 0.001$, NS: Nonsignificant)

the mechanical properties of the single-pore scaffold with HA particles was higher than the dual-pore scaffold without HA particles and the dual-pore scaffold with HA particles, in contrast to the trend in porosities (Fig. 3(b)).

To indirectly assess cell activity including cell adhesion and proliferation in the fabricated scaffolds, the level of water absorption of the fabricated scaffolds was measured (Fig. 3(c)). The water absorption capacity of a scaffold is related to the level of cell proliferation because the absorbed water influences the supply of nutrients to the cells.[32,33] The water absorption of the single-pore scaffold with HA particles, the dual-pore scaffold without HA particles, and the dual-pore scaffold with HA particles was measured to be 133.7±2.3%, 184.5±1.1%, and 220.6± 0.5%, respectively. The dual-pore structure, which increases porosity, influenced the water absorption capacity of the scaffolds, and the existence of exposed HA, which is hydrophilic, also increased water absorption.

3.3 Analysis of cell culture characteristics

To assess the cell adhesion, proliferation and viability of the fabricated scaffolds, CCK-8 assay, DNA contents, and Live/Dead stain investigations were performed using Saos-2 cells over a period of two weeks. As shown in Fig. 4(a) after one day, the cell adhesion of the dual-pore scaffold without HA particles and the dual-pore scaffold with HA particles was higher than that of the single-pore scaffold with HA particles. Moreover, the cell adhesion of the dual-pore scaffold without HA particles was similar to that of the dual-pore scaffold with HA particles. This result suggests that the dual-pore structure effectively influenced cell adhesion, compared with the existence of HA particles with hydrophilic characteristics. Furthermore, the proliferation of cells in the dual-pore scaffold without HA particles and the dual-pore scaffold with HA particles after 14 days was significantly better than that of the single-pore scaffold with HA particles. As depicted in Fig. 4(a) after 14 days, the absorbance of the dual-pore scaffold with HA particles was higher than that of the dual-pore scaffold without HA particles.

Additionally, to quantify the cell-proliferation in the scaffold, the DNA contents of the cultured cells were measured at 1, 7, and 14 days (Fig. 4(b)). For the single-pore scaffold and both types of dual-pore scaffolds, the trend in DNA content was similar to that of the CCK-8 assay. However, for the dual-pore scaffold without HA particles and the dual-pore scaffold with HA particles, the trend in DNA content was different than that of the CCK-8 assay.

As shown in Fig. 4(b), the difference between the dual-pore scaffold without HA particles and the dual-pore scaffold with HA particles was non-significant at 1, 7, and 14 days. This result can be explained as follows. Although the existence of HA particles influenced the vitality of cells due to the release of calcium ions and phosphorus ions, the dual-pore structure had the dominant influence on the manner of adhesion and the proliferation of osteoblast-like cells, compared with HA (osteoconductive and hydrophilic) particles. Moreover, as shown in Fig. 5, the viability results were similar to those obtained for DNA content.

Consequently, the results of the CCK-8 assay, DNA content, and Live/Dead stain tests demonstrated that the dual-pore structure effectively improved the scaffold's osteoblast-like cell's adhesion and proliferation abilities, compared with the existence of HA particles, which have

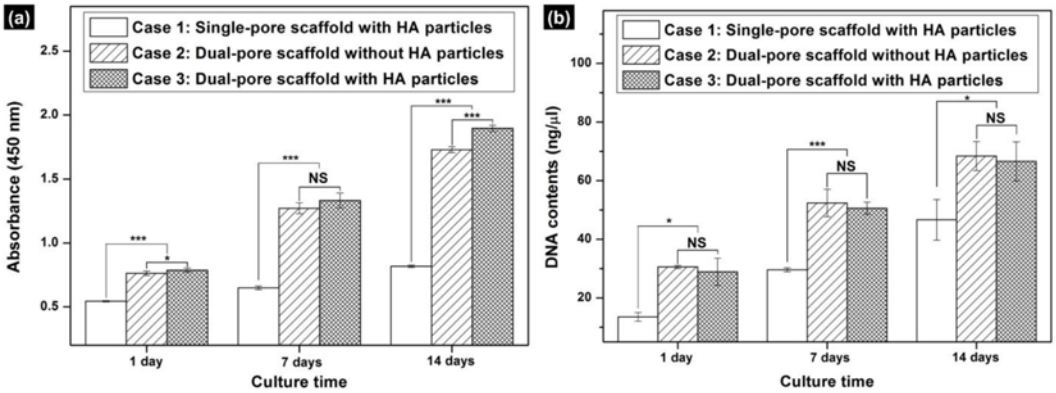

Fig. 4 CCK-8 and DNA content results for Saos-2 cells cultured on fabricated scaffolds after 2 weeks: (a) CCK-8 assay and (b) DNA contents of the single-pore scaffold with HA particles, the dual-pore scaffold without HA particles, and the dual-pore scaffold with HA particles. (*p < 0.05, ***p < 0.001, NS: Nonsignificant)

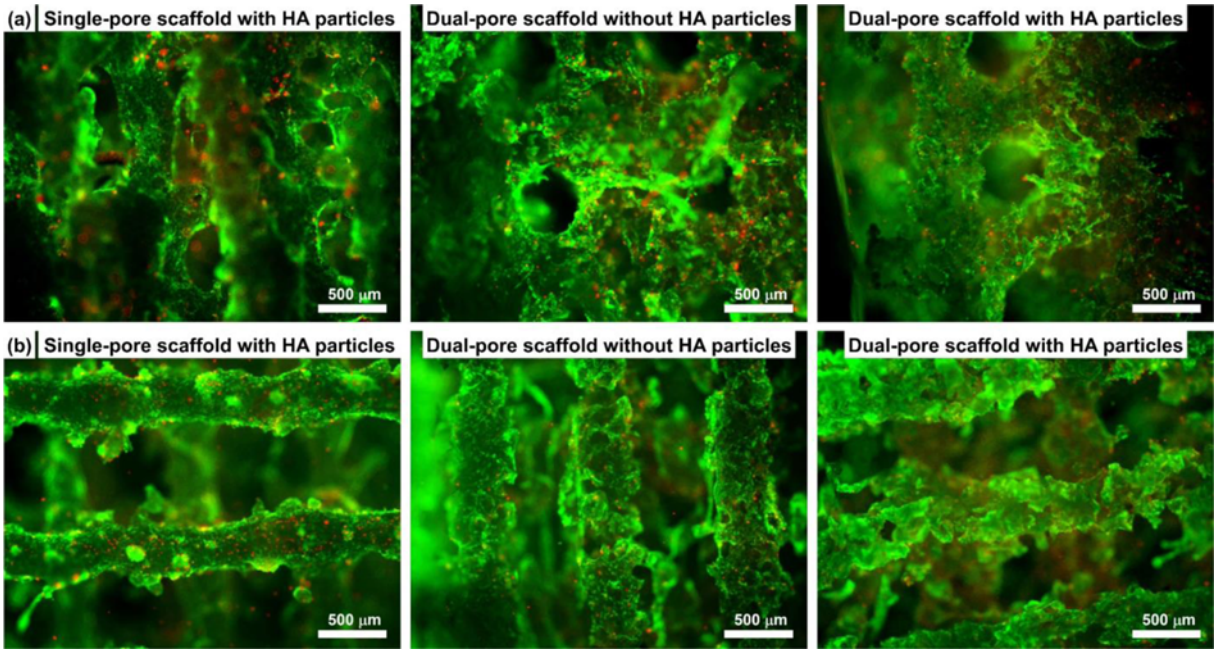

Fig. 5 Observation of live and dead stains: (a) stain images at 7 days after cultivation of seeded (osteoblast-like) Saos-2 cells and (b) stain images at 14 days after cultivation of seeded (osteoblast-like) Saos-2 cells of the single-pore scaffold with HA particles, the dual-pore scaffold without HA particles, and the dual-pore scaffold with HA particles

hydrophilic and ion release characteristics.

4. Conclusions

In this study, to compare the effectiveness of the dual-pore structure and hydroxyapatite to enhance the proliferation of osteoblast-like cells, well-interconnected dual-pore scaffolds with/without HA particles, and single-pore scaffolds with HA particles, were fabricated using a combination of SLUP (Salt-Leaching Using Powder) and WNM (Wire-Network Molding) techniques. To exclude the morphological influence of the fabricated scaffolds on cell activity, the single-pore scaffold with HA particles, the dual-pore scaffold without HA particles, and the dual-pore scaffold with HA particles were fabricated using the same manufacturing process and weight ratio of NaCl/HA particles.

According to our results, the effect of the dual-pore structure on the osteoblast-like cell's adhesion and proliferation was higher than that of HA particles in the scaffold, because it enhanced the amount of living space and the availability of nutrients/oxygen to the cells. Furthermore, although the existence of HA particles in the scaffolds increased cell vitality, the HA particles did not significantly affect the overall cell proliferation as compared with the dual-pore structure.

Consequently, we verified that the existence of the dual-pore structure was the dominant influence in the osteoblast-like cell's adhesion and proliferation compared with the existence of HA particles. In future studies, we are going to verify our proposed hypothesis with detail-designed experiments focused on the scaffold's manufacturing method, pore size, dual-pore proportion, and HA content.

ACKNOWLEDGEMENT

This work was supported by Wonkwang University in 2016.

REFERENCES

1. Akbarzadeh, R., Minton, J. A., Janney, C. S., Smith, T. A., James, P. F., and Yousefi, A.-M., "Hierarchical Polymeric Scaffolds Support the Growth of MC3T3-E1 Cells," Journal of Materials Science: Materials in Medicine, Vol. 26, No. 2, Paper No. 116, 2015.
2. Cancedda, R., Dozin, B., Giannoni, P., and Quarto, R., "Tissue Engineering and Cell Therapy of Cartilage and Bone," Matrix Biology, Vol. 22, No. 1, pp. 81-91, 2003.
3. Hollister, S. J., Maddox, R. D., and Taboas, J. M., "Optimal Design and Fabrication of Scaffolds to Mimic Tissue Properties and Satisfy Biological Constraints," Biomaterials, Vol. 23, No. 20, pp. 4095-4103, 2002.
4. Wei, C. and Dong, J., "Hybrid Hierarchical Fabrication of Three-Dimensional Scaffolds," Journal of Manufacturing Processes, Vol. 16, No. 2, pp. 257-263, 2014.
5. Seyednejad, H., Gawlitta, D., Kuiper, R. V., de Bruin, A., van Nostrum, C. F., et al., "In Vivo Biocompatibility and Biodegradation of 3D-Printed Porous Scaffolds Based on a Hydroxyl-Functionalized Poly (ε-Caprolactone)," Biomaterials, Vol. 33, No. 17, pp. 4309-4318, 2012.
6. Heo, S. J., Kim, S. E., Wei, J., Hyun, Y. T., Yun, H. S., et al., "Fabrication and Characterization of Novel Nano- and Micro-HA/PCL Composite Scaffolds Using a Modified Rapid Prototyping Process," Journal of Biomedical Materials Research Part A, Vol. 89, No. 1, pp. 108-116, 2009.
7. Ding, X., Wei, X., Huang, Y., Guan, C., Zou, T., et al., "Delivery of Demineralized Bone Matrix Powder Using a Salt-Leached Silk Fibroin Carrier for Bone Regeneration," Journal of Materials Chemistry B, Vol. 3, No. 16, pp. 3177-3188, 2015.
8. Thein-Han, W. W., and Xu, H. H. K., "Prevascularization of a Gas-Foaming Macroporous Calcium Phosphate Cement Scaffold via Coculture of Human Umbilical Vein Endothelial Cells and Osteoblasts," Tissue Engineering Part A, Vol. 19, No. 15-16, pp. 1675-1685, 2013.
9. Taherkhani, S. and Moztarzadeh, F., "Fabrication of a Poly (ε-Caprolactone)/Starch Nanocomposite Scaffold with a Solvent-Casting/Salt-Leaching Technique for Bone Tissue Engineering Applications," Journal of Applied Polymer Science, Vol. 133, No. 23, Paper No. 43523, 2016.
10. Yu, N. Y., Schindeler, A., Peacock, L., Mikulec, K., Fitzpatrick, J., et al., "Modulation of Anabolic and Catabolic Responses via a Porous Polymer Scaffold Manufactured Using Thermally Induced Phase Separation," European Cells and Materials, Vol. 25, pp. 190-203, 2013.
11. Nie, L., Chen, D., Suo, J., Zou, P., Feng, S., et al., "Physicochemical Characterization and Biocompatibility in Vitro of Biphasic Calcium Phosphate/Polyvinyl Alcohol Scaffolds Prepared by Freeze-Drying Method for Bone Tissue Engineering Applications," Colloids and Surfaces B: Biointerfaces, Vol. 100, pp. 169-176, 2012.
12. Weng, L., Teusink, M. J., Shuler, F. D., Parecki, V., and Xie, J., "Highly Controlled Coating of Strontium-Doped Hydroxyapatite on Electrospun Poly (ε-Caprolactone) Fibers," Journal of Biomedical Materials Research Part B: Applied Biomaterials, Vol. 105, No. 4, pp. 753-763, 2017.
13. Ronca, A., Ambrosio, L., and Grijpma, D. W., "Preparation of Designed Poly (D, L-Lactide)/Nanosized Hydroxyapatite Composite Structures by Stereolithography," Acta biomaterialia, Vol. 9, No. 4, pp. 5989-5996, 2013.
14. Shuai, C., Gao, C., Nie, Y., Hu, H., Zhou, Y., and Peng, S., "Structure and Properties of Nano-Hydroxypatite Scaffolds for Bone Tissue Engineering with a Selective Laser Sintering System," Nanotechnology, Vol. 22, No. 28, Paper No. 285703, 2011.
15. Luo, Y., Lode, A., Wu, C., Chang, J., and Gelinsky, M., "Alginate/Nanohydroxyapatite Scaffolds with Designed Core/Shell Structures Fabricated by 3D Plotting and in situ Mineralization for Bone Tissue Engineering," ACS Applied Materials & Interfaces, Vol. 7, No. 12, pp. 6541-6549, 2015.
16. Kang, H.-W., Rhie, J.-W., and Cho, D.-W., "Development of a Bi-Pore Scaffold Using Indirect Solid Freeform Fabrication Based on Microstereolithography Technology," Microelectronic Engineering, Vol. 86, Nos. 4-6, pp. 941-944, 2009.
17. Park, K., Jung, H. J., Son, J. S., Park, K. D., Kim, J. J., et al., "Preparation of Biodegradable Polymer Scaffolds with Dual Pore System for Tissue Regeneration," Macromolecular Symposia, Vols. 249-250, No. 1, pp. 145-150, 2007.
18. Mohanty, S., Sanger, K., Heiskanen, A., Trifol, J., Szabo, P., et al., "Fabrication of Scalable Tissue Engineering Scaffolds with Dual-Pore Microarchitecture by Combining 3D Printing and particle Leaching," Materials Science and Engineering: C, Vol. 61, pp. 180-189, 2016.
19. Park, S. H., Kim, T. G., Kim, H. C., Yang, D.-Y., and Park, T. G., "Development of Dual Scale Scaffolds Via Direct Polymer Melt Deposition and Electrospinning for Applications in Tissue Regeneration," Acta Biomaterialia, Vol. 4, No. 5, pp. 1198-1207, 2008.
20. Rizzi, S. C., Heath, D., Coombes, A., Bock, N., Textor, M., and Downes, S., "Biodegradable Polymer/Hydroxyapatite Composites: Surface Analysis and Initial Attachment of Human Osteoblasts," Journal of Biomedical Materials Research Part A, Vol. 55, No. 4, pp. 475-486, 2001.
21. Thuaksuban, N., Luntheng, T., and Monmaturapoj, N., "Physical Characteristics and Biocompatibility of the Polycaprolactone-Biphasic Calcium Phosphate Scaffolds Fabricated Using the Modified Melt Stretching and Multilayer Deposition," Journal of Biomaterials

Applications, Vol. 30, No. 10, pp. 1460-1472, 2016.

22. Seol, Y.-J., Park, J. Y., Jung, J. W., Jang, J., Girdhari, R., et al., "Improvement of Bone Regeneration Capability of Ceramic Scaffolds by Accelerated Release of their Calcium Ions," Tissue Engineering Part A, Vol. 20, Nos. 21-22, pp. 2840-2849, 2014.
23. Cho, Y. S., Hong, M. W., Kim, S.-Y., Lee, S.-J., Lee, J. H., et al., "Fabrication of Dual-Pore Scaffolds Using SLUP (Salt Leaching Using Powder) and WNM (Wire-Network Molding) Techniques," Materials Science and Engineering: C, Vol. 45, pp. 546-555, 2014.
24. Cho, Y. S., Hong, M. W., Jeong, H. J., Lee, S. J., Kim, Y. Y., and Cho, Y. S., "The Fabrication of Well-Interconnected Polycaprolactone/ Hydroxyapatite Composite Scaffolds, Enhancing the Exposure of Hydroxyapatite Using the Wire-Network Molding Technique," Journal of Biomedical Materials Research Part B: Applied Biomaterials, Vol. 105, No. 8, pp. 2315-2325, 2017.
25. Chen, G., Zhou, P., Mei, N., Chen, X., Shao, Z., et al., "Silk Fibroin Modified Porous Poly (ε-Caprolactone) Scaffold for Human Fibroblast Culture in Vitro," Journal of Materials Science: Materials in Medicine, Vol. 15, No. 6, pp. 671-677, 2004.
26. Li, X., Shi, J., Dong, X., Zhang, L., and Zeng, H., "A Mesoporous Bioactive Glass/Polycaprolactone Composite Scaffold and Its Bioactivity Behavior," Journal of Biomedical Materials Research Part A, Vol. 84, No. 1, pp. 84-91, 2008.
27. Oh, S. H., Kang, S. G., Kim, E. S., Cho, S. H., and Lee, J. H., "Fabrication and Characterization of Hydrophilic Poly (Lactic-Co-Glycolic Acid)/Poly (Vinyl Alcohol) Blend Cell Scaffolds by Melt-Molding Particulate-Leaching Method," Biomaterials, Vol. 24, No. 22, pp. 4011-4021, 2003.
28. Oh, S. H., Kang, S. G., and Lee, J. H., "Degradation Behavior of Hydrophilized PLGA Scaffolds Prepared by Melt-Molding Particulate-Leaching Method: Comparison with Control Hydrophobic One," Journal of Materials Science: Materials in Medicine, Vol. 17, No. 2, pp. 131-137, 2006.
29. Makaya, K., Terada, S., Ohgo, K., and Asakura, T., "Comparative Study of Silk Fibroin Porous Scaffolds Derived from Salt/Water and Sucrose/Hexafluoroisopropanol in Cartilage Formation," Journal of Bioscience and Bioengineering, Vol. 108, No. 1, pp. 68-75, 2009.
30. Oh, S. H., Park, S. C., Kim, H. K., Koh, Y. J., Lee, J.-H., et al., "Degradation Behavior of 3D Porous Polydioxanone-b-Polycaprolactone Scaffolds Fabricated Using the Melt-Molding Particulate-Leaching Method," Journal of Biomaterials Science, Polymer Edition, Vol. 22, Nos. 1-3, pp. 225-237, 2011.
31. Gere, J. M., "Mechanics of Materials," Thomson, 6th Ed. 2004.
32. Hong, S. and Kim, G., "Fabrication of Electrospun Polycaprolactone Biocomposites Reinforced with Chitosan for the Proliferation of Mesenchymal Stem Cells," Carbohydrate Polymers, Vol. 83, No. 2, pp. 940-946, 2011.
33. Lee, H., Yeo, M., Ahn, S., Kang, D. O., Jang, C. H., et al., "Designed Hybrid Scaffolds Consisting of Polycaprolactone Microstrands and Electrospun Collagen-Nanofibers for Bone Tissue Regeneration," Journal of Biomedical Materials Research Part B: Applied Biomaterials, Vol. 97, No. 2, pp. 263-270, 2011.
34. Shen, H., Hu, X., Yang, F., Bei, J., and Wang, S., "An Injectable Scaffold: RhBMP-2-Loaded Poly (Lactide-Co-Glycolide)/ Hydroxyapatite Composite Microspheres," Acta Biomaterialia, Vol. 6, No. 2, pp. 455-465, 2010.